Multiscale Review of the Development and Early Evolution of the 9 April 1991 Derecho

JAMES W. DUKE AND JOSEPH A. ROGASH

National Weather Service, Memphis, Tennessee

(Manuscript received 6 January 1992, in final form 13 August 1992)

ABSTRACT

A case study was conducted of the development and early evolution of a severe squall line that occurred 9 April 1991. The squall line formed near the border between Arkansas and Tennessee, then raced toward the northeast during the next 14 hours. Damaging winds were widespread with the squall line; thus, the 9 April 1991 event fits the definition of a derecho. Radar observations of the evolving squall line show signatures often correlated with damaging surface winds, including a bow echo, strong reflectivity gradients, and weak echo channels. Synoptic conditions under which the 9 April 1991 event occurred were significantly different in many respects from those associated with warm-season derechos. Differences include absence of important low-altitude signatures and more vigorous weather systems. There were similarities to the warm-season pattern, however, including moderately strong winds aloft, a very unstable thermodynamic profile, and cool dry air at midlevels. The similarities suggest refinements of the derecho model.

1. Introduction

A severe convective windstorm developed near the Arkansas–Tennessee border early on 9 April 1991. The storm began as an elongated area of thunderstorms over central Arkansas between 0900 and 1000 UTC and evolved into an extensive squall line as it moved east, and a large bow echo (Fujita 1978) became the dominant squall-line pattern shown by radar. The 9 April 1991 storm was especially intense and long-lived. It brought damaging wind, hail, and a few tornadoes to parts of at least eight states as it swept toward the east-northeast. Destructive winds continued more than 14 h after the squall line became organized around 1300 UTC—until after 0200 UTC 10 April 1991. The National Severe Storms Forecast Center (NSSFC) logged more damaging weather reports from the 9–10 April 1991 occurrence than on any other date in the center's history (Johns 1991, personal communication). Figure 1 shows damaging weather reported between 1200 and 1900 UTC.

Johns and Hirt (1987) have adopted Gustavus Hinrichs' "derecho" label for this type of long-lived, convectively driven severe windstorm (*derecho* is a Spanish word meaning direct, or straight ahead). Further, Johns and Hirt (1987) and Johns et al. (1990) have provided extensive information about conditions under which warm-season (May through August) derechos form. Others (Przybylinski and DeCaire 1985; Smith 1990; Burgess and Smull 1990; Johns and Leftwich 1988) have reviewed other aspects of derecho evolution during the warm season.

The 9 April 1991 synoptic environment did not appear to favor derecho formation (Johns and Hirt 1987; Johns et al. 1990); thus, the event had begun before forecasters recognized the widespread threat. Development of a major derecho when the 9 April 1991 synoptic patterns seemed unfavorable suggests derechos can form under conditions other than those common to warm-season events.

Since existing studies describe derechos that have occurred in the warm season, they do not provide a general model against which to compare the 9 April 1991 (transition season) event. Thus, the 9 April 1991 event provides a unique chance to examine features and patterns associated with a non-warm-season derecho, and to compare those parameters with those associated with warm-season derechos. This paper will discuss synoptic and mesoscale weather associated with formation and early evolution of the 9 April 1991 squall line and derecho, and compare them with conditions associated with warm-season derechos.

The comparison finds major differences in several important meteorological parameters, and finds similarities in several other meteorological parameters (Table 1). The differences and similarities may have forecast implications for other non-warm-season derecho situations.

2. Data and analysis procedures

Surface and upper-air data are from the National Weather Service (NWS) Automation of Field Offices and Services (AFOS) and the NWS Service Records

Corresponding author address: James W. Duke, NOAA/NWSFO, 7777 Walnut Grove Road-OM1, Memphis, TN 38120-2198.

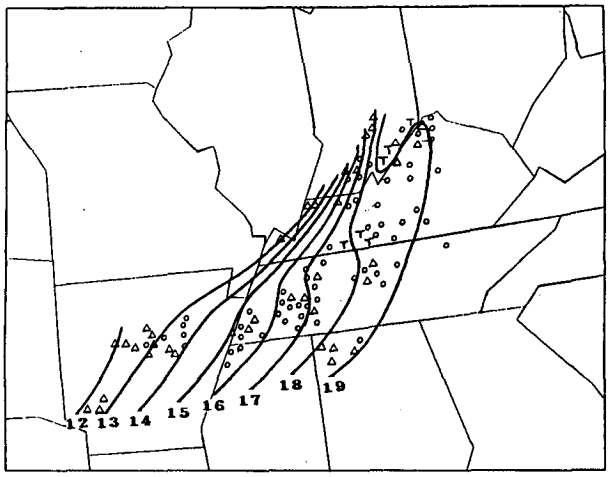

FIG. 1. Isochrones (hours UTC) of severe weather (National Weather Service defines a severe thunderstorm as one that produces a tornado, 1.9-cm hail, and/or 26 m s^{-1} wind gusts) occurrence during early evolution of 9 April 1991 derecho (1000 to 1900 UTC). Triangles are large hail events, circles are damaging wind reports, and *T* indicates tornado.

Retention System. Manual analysis, using altimeter setting (reduced to millibars) for surface pressure, was performed from hourly surface aviation observations. Continuity helped locate some features on the hourly maps, especially outflow boundaries. This was necessary since the spatial density of reports was often inadequate to support accurate analysis using single maps independently. Surface data were also processed using the AFOS Data Analysis Program (Bothwell 1985).

Upper-air data were manually analyzed for the standard (850 mb, 700 mb, 500 mb, 300 mb, 250 mb, and 200 mb) levels at 1200 UTC. Heights were contoured each 15 m, and isotherms drawn every 2°C. Isodrosotherms were drawn every 3°C at 850 mb, and dewpoint depression was analyzed at 700 mb (not shown) and 500 mb.

Individual rawinsonde observations were analyzed using automated procedures commonly available at NWS sites. These include the convection parameters and hodograph program (Stone 1988) and the SHARP workstation (Hart and Korotky 1991) program. Both provide a variety of stability indices and assorted other objective measures of the thermodynamic structure of the atmosphere (K-Index, SELS Lifted Index, equilibrium level, cap strength, etc.). Sounding kinematics were also analyzed for derived wind and shear values such as bulk Richardson number, indicated storm motion, and helicity.

Surface equivalent potential temperature (θ_e) analyses were made using data from hourly aviation observations. A cross section of θ_e covering approximately the west half of the derecho's main path of destruction was constructed using surface and upper-air data from 1200 UTC.

Plan position indicator (PPI) data from NWS 10-cm radars at Memphis, Tennessee, and Nashville, Tennessee, were compiled from archive film and re-

TABLE 1. 9 April 1991 meteorological parameters compared to those associated with warm-season derechos.

Parameter	Typical warm-season event	9 April 1991 transition-season event
Surface boundary	East–west front	Approaching cold front
Surface moisture	Pooled along and south of surface boundary with maximum near midpoint of derecho track	Moisture ridge, no pooling
Surface wind	Light, mainly south to southwest	Light, mainly southerly
Surface θ_e	Greater than 360 K along much of derecho path	Near 340 K over genesis area, decreasing along track
Approaching midlevel trough	Weak	Vigorous
500-mb moisture	Dry, $T - T_d = 22$°C at midpoint	Dry, $T - T_d = 10$°C over genesis area, drier downstream toward midpoint
500-mb temperature	−10°C	−15°C
500-mb wind	21 m s^{-1}	26 m s^{-1}
700-mb moisture	$T - T_d = 14$°C at midpoint	$T - T_d > 10$°C
700- and 850-mb warm advection	Maximum over genesis area with weaker advection east along track	Maximum just east of genesis area
850-mb moisture	Pooled along derecho track; highest values near midpoint	Moisture ridge with highest values over the west half of the track
CAPE	2400 J kg^{-1} over genesis area, 4500 at midpoint	2200 to 2500 J kg^{-1} over genesis area and just downstream, but decreasing downstream
Level of free convection	Slopes downward from genesis area to midpoint	Slopes downward eastward from genesis area
Bulk Richardson number	Supports bow-echo formation	Supports bow echo and squall-line formation
Derecho movement	Along 700- and 850-mb thermal gradient, just north of thermal ridge	Slightly across gradient toward warmer air in thermal ridge

flectivity contours were projected onto regional maps. The PPI information gave an excellent depiction of the radar echo shape and location. While quality of the archive film was not good enough to allow precise resolution of the strongest reflectivity gradients, storm location and appearance were representative of that observed during the event.

3. 9 April 1991 synoptic and mesoscale conditions compared to typical warm-season derecho conditions

North American 300-mb circulation (Fig. 2a) at 1200 UTC 9 April 1991 is dominated by a vigorous trough. Its axis extends through North Dakota southward into western Oklahoma. This strong disturbance is moving east across the central plains toward the Mississippi valley. The derecho genesis area (central Arkansas and west Tennessee) is located in a part of the circulation often considered favorable for severe weather (Miller 1972): where winds are strong and diffluent just east of an approaching trough.

The location and amplitude of the trough at 500 mb (Fig. 2b) is similar to 300 mb. Winds show distinct cyclonic curvature along the trough axis, with slightly anticyclonic flow over the derecho genesis area. A narrow zone of small temperature–dewpoint depression is just east of the trough. The increased moisture suggests large-scale lifting ahead of the disturbance. Temperature–dewpoint depressions are progressively larger east of the trough, around 10°C over the genesis area, and near 30°C along the derecho track. Strong cold-air advection at 500 mb is north of the derecho genesis area, but weak cold advection is occurring over Arkansas and west Tennessee. Relatively cold temperatures for the season, near −15°C, cover most of the south-central United States; that is about 5°C colder than for typical summertime derechos (Johns et al. 1990).

Warm-season derechos (Johns et al. 1990) form just ahead of a weak midtropospheric shortwave trough. And, unlike the 9 April 1991 event, warm-season derechos occur in regions where the lower and middle troposphere have a weak temperature gradient. Pronounced 850-mb warm advection is occurring on southwest winds over the 9 April 1991 derecho genesis area (Fig. 3a). Abundant moisture is present over the genesis area, with 850-mb dewpoints at least 10°C. The 850-mb thermal pattern is highly baroclinic—temperatures range from 19°C in northeast Texas to −1°C in southwest Nebraska.

Surface features associated with warm-season derechos (Johns and Hirt 1987; Johns et al. 1990) almost invariably include an east–west surface boundary. There is no east–west boundary on 9 April 1991. The most significant surface feature at 1200 UTC (Fig. 3b) is a strong cold front extending from Illinois through north-central and southwest Arkansas. East of the front,

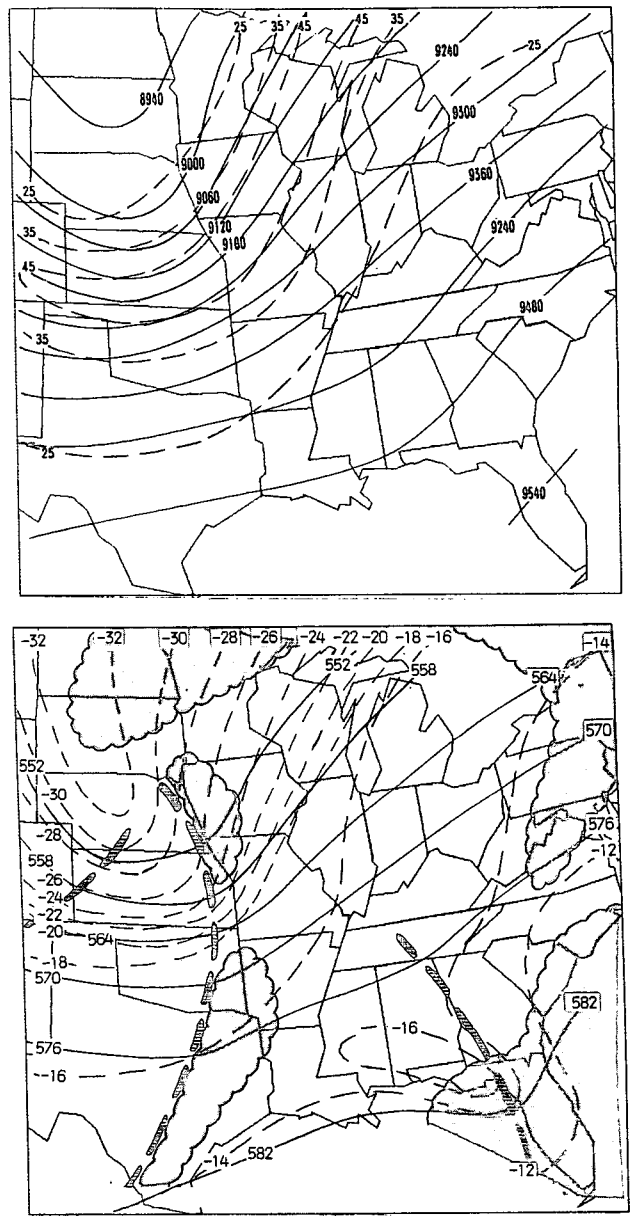

FIG. 2. (a) 1200 UTC 9 April 1991 300-mb analysis. Solid lines are isoheights (meters), dashed lines are isotachs (m s^{-1}). (b) 1200 UTC 9 April 1991 500-mb analysis. Solid lines are isoheights (decameters), light dashed lines are isotherms (°C), heavy dashed lines are trough axes. Stippled areas show locations of $T - T_d < 6$°C.

southwest winds near 5 m s^{-1} are carrying warm air into the lower and central Mississippi valleys.

Temperatures in the warm sector are 6° to 12°C higher than normal for this time of day. Similarly, dewpoints are abnormally high—between 10° and 15°C—and form a dewpoint ridge that extends northward into the genesis area. In contrast, lower-tropospheric moisture associated with summertime derechos is often pooled along and south of the boundary with

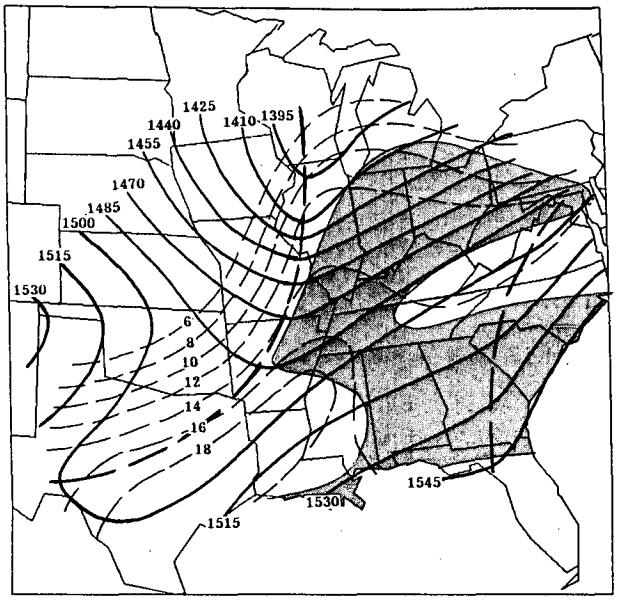

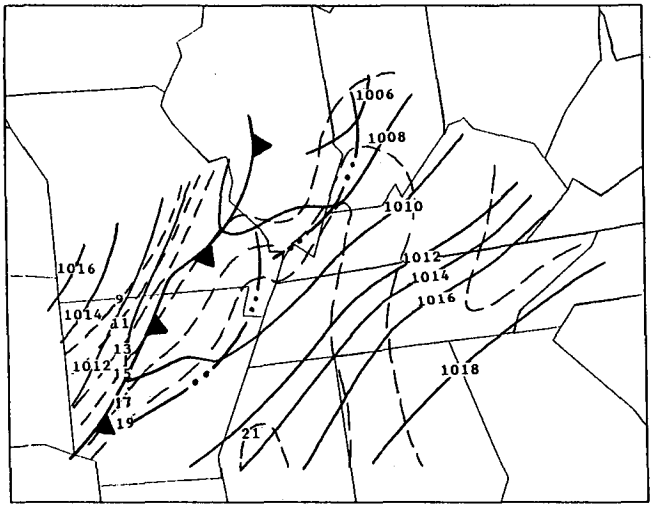

FIG. 3. (a) 1200 UTC 9 April 1991 850-mb analysis. Solid lines are isoheights (meters), light dashed lines are isotherms (°C), heavy dashed lines are trough axes. Stippled areas show locations of T_d > 9°C. (b) 1200 UTC 9 April 1991 surface analysis. Solid lines are isobars, drawn every 2 mb. Dashed lines are isodrotherms, drawn every 2°C. Dash-double-dot-dash lines mark surface outflow boundary locations.

a maximum near the midpoint of the derecho track (Johns and Hirt 1987; Johns et al. 1990).

Surface moisture convergence at 1100 UTC (Fig. 4) confirms existence of a direct circulation created by the thermodynamic gradient (Shapiro 1982). Surface equivalent potential temperatures at 1200 UTC (Fig. 5) show a very strong thermodynamic gradient across the front. Location of convergence values up to 160 g kg^{-1} h^{-1} suggests low-level forcing was the primary trigger for the severe thunderstorms in progress at that time.

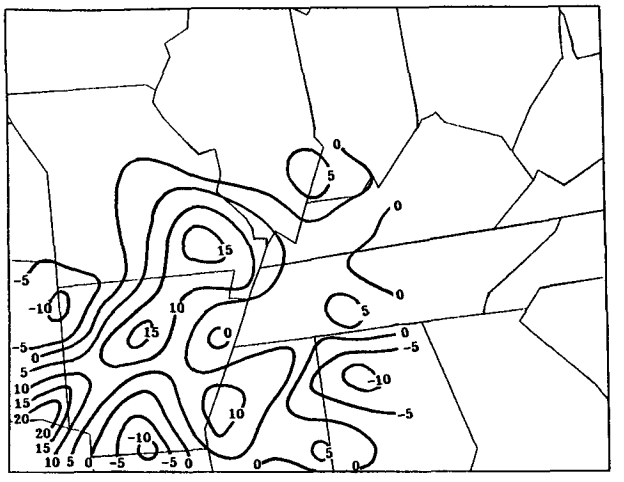

FIG. 4. 1100 UTC 9 April 1991 surface moisture convergence (g kg^{-1} h^{-1} × 10^{-1}).

Tropospheric temperature patterns at 1200 UTC show a convectively unstable thermodynamic profile over the derecho genesis area (Figs. 6a and 6b). Cool dry air is present in the middle troposphere with warm moist air at lower levels. SELS lifted indices are −6 to −9, and mixing ratios average 14 g kg^{-1}. The level of free convection (LFC) slopes downward, from around 750 mb at Little Rock to nearly 900 mb at Paducah.

Convectively available potential energy (CAPE) ranges from 2233 J kg^{-1} at Little Rock to 2766 J kg^{-1} at Paducah. Similarly, total totals are extremely high: 59 at Paducah and 58 at Little Rock. Bulk Richardson numbers (Ri), ratios of CAPE and vertical wind shear (Fig. 6c), are 117 at Little Rock and 54 at Paducah. Weisman and Klemp (1984) find multicellular convection associated with Ri > 40. Large amounts of

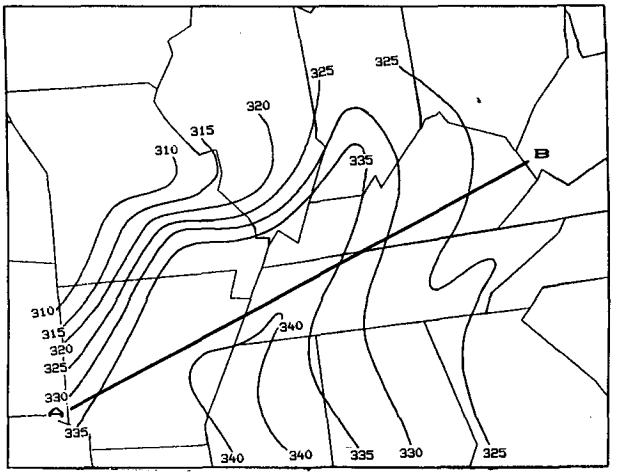

FIG. 5. 1200 UTC 9 April 1991 surface equivalent potential temperature θ_e. Line connecting points A and B is near main damage path during derecho development and early evolution.

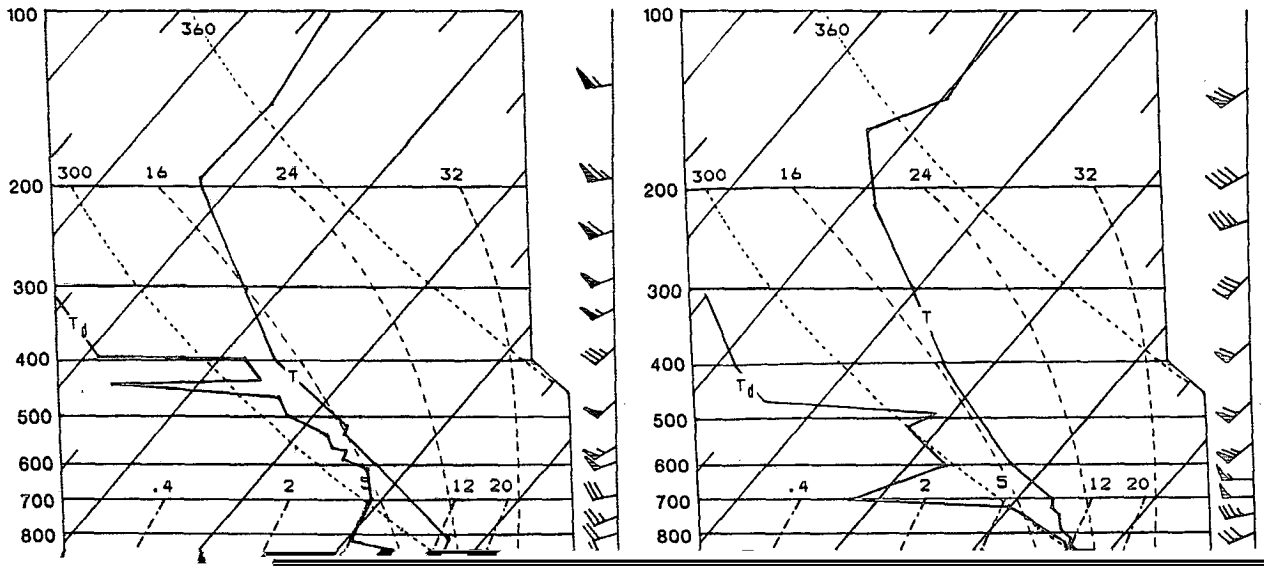
100
200
300
400
500
600
700
800
360
300
16
24
32
T_d
T
.4
2
5
12
20

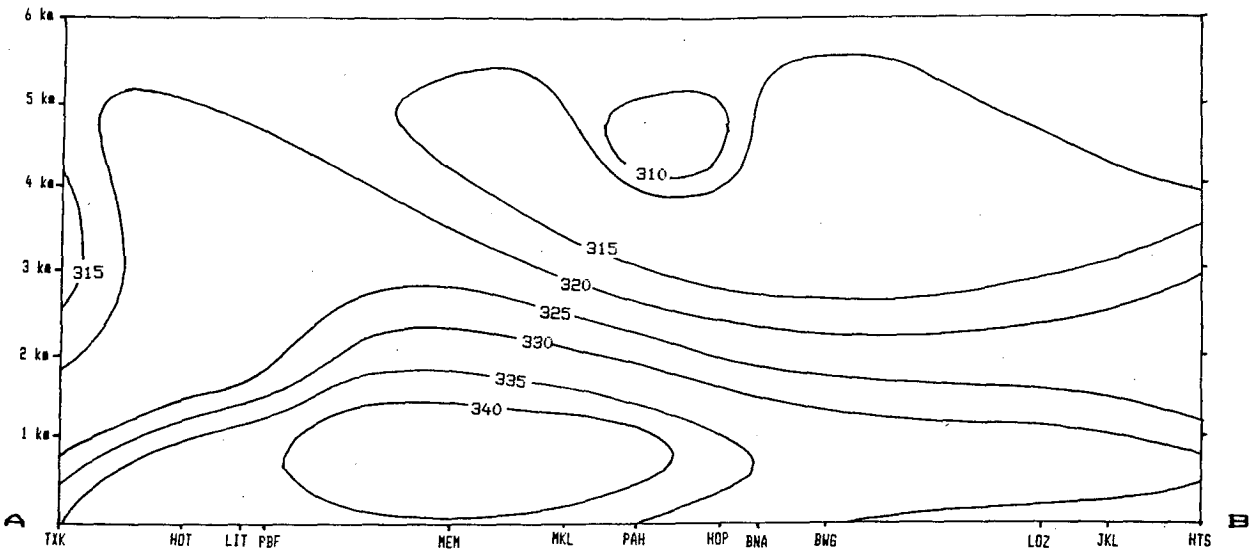

FIG. 7. 1200 UTC 9 April 1991 cross section of equivalent potential temperature (θ_e). Points A and B (left and right margins) are at the southwest and northeast ends of damage swath during derecho formation and early evolution.

derecho genesis areas. The moist low levels with warm advection in the lower troposphere make instability values high. SELS lifted indices associated with warm-season events are mostly between −4 and −11; CAPE is between 2600 and 6300 J kg^{-1}, with the highest values around the midpoint of the derecho track (Johns and Hirt 1987; Johns et al. 1990).

Winds observed by the Little Rock 1200 UTC rawinsonde on 9 April 1991 veer about 30° between the surface and 4 km. Wind speeds diminish from 17 m s^{-1} at 500 m AGL to only 10 m s^{-1} at 1500 m AGL, then gradually increase to around 25 m s^{-1} at 4 km AGL (Fig. 6c). Downstream at Paducah, winds veered about 40° between the surface and 2 km AGL with nearly undirectional winds above. The unidirectional shear was greater than at Little Rock, increasing from 16 m s^{-1} at 500 m AGL to 30 m s^{-1} at 4 km (Fig. 6c).

Isolated supercell thunderstorms sometimes characterize the beginning of warm-season derechos (Johns and Leftwich 1988), but forerunner convection can also be multicellular (Burgess and Smull 1990). Regardless of the initial characteristics, a squall line (bow echo) quickly becomes the dominant structure. The evolution seems to occur, as it did in this springtime event, as the thunderstorms move into a region where the LFC becomes progressively lower, and from an environment where winds veer with height to an environment with predominantly unidirectional shear (Johns and Leftwich 1988).

4. Early derecho evolution shown by radar PPI information

Derechos are products of very long-lived squall lines, squall lines that produce destructive winds throughout their lifetime. The squall line's long life and its ability to produce damaging wind appear to be functions of instability and the vertical distribution of moisture and wind shear (Weisman 1990). Numerical simulations (Klemp et al. 1985; Weisman and Klemp 1986; Weis-

TABLE 2. 9 April 1991 1200 UTC mean wind vectors based on 240°/23 m s^{-1} storm motion.

	Paducah		Little Rock	
Depth AGL (m)	Mean ground-relative wind vector (Dir/m s^{-1})	Mean storm-relative wind vector (Dir/m s^{-1})	Mean ground-relative wind vector (Dir/m s^{-1})	Mean storm-relative wind vector (Dir/m s^{-1})
1000	217/9	74/15	243/11	58/12
2000	235/12	65/11	247/11	55/13
3000	239/13	61/10	249/11	52/12
4000	247/15	47/8	250/13	49/10
5000	245/18	46/6	247/15	49/8
6000	242/20	48/4	244/16	51/7

man et al. 1990) show that moderate to strong unidirectional shear at low levels, with weak shear at middle and upper levels, is critical to the production of strong, long-lived squall lines. That condition existed at 1200 UTC 9 April 1991 (Fig. 6c). Strong unidirectional shear was present in the subcloud layer (below 1 km), and between 2 and 4.5 km at 1200 UTC 9 April 1991. Only weak shear was present above 4.5 km.

The storm-relative wind profile may be more critical to squall-line evolution than the initial ambient wind (Smull and Houze 1987; Gao and Zhang 1989; Klemp et al. 1985; Schmidt et al. 1990; Xue 1990). The 1200 UTC winds suggest storms would move toward the east-northeast at 13 to 18 m s^{-1} (Miller 1972). Between 1200 and 1800 UTC, however, the squall line moved from the southwest (240°), but at 20 to 25 m s^{-1}. Thus, squall-line movement, though toward the east-northeast, was 165% of the speed indicated by the ambient flow. The fast movement created a storm-relative flow (based on 1200 UTC wind data) directed from in front of the squall line to its rear (Table 2).

Figures 8a through 8j are a series of tracings of archive PPI film from NWS 10-cm radars at Memphis, Tennessee, and Nashville, Tennessee. Figures 8a through 8e are from the WSR-74S radar at Memphis. Figures 8g through 8j are from the WSR-57 radar at Nashville. Figure 8f is a composite from both radars. Contours represent NWS Video Integrator Processor (VIP) levels, but archive film quality was inadequate to allow precise location of the highest VIP levels.

Only considerable imagination finds a linear feature in the isolated echoes over Arkansas at 1056 UTC (Fig. 8a). A northeast–southwest line is evident at 1153 UTC (Fig. 8b) though, and there is a hint of a line echo wave pattern (LEWP) from just west of Little Rock, southward. Wind gusts to 25 m s^{-1} and 4.5-cm-diameter hail were occurring with the intense echo located near the crest of the possible LEWP, 40 km west-northwest of Little Rock.

An elongated cluster of intense echoes that extends northeast–southwest just east of Little Rock dominates the radar pattern at 1257 UTC (Fig. 8c). Damaging winds (up to 26 m s^{-1}) were in progress with several of these echoes, but the size and frequency of hail occurrence decreased; maximum hail diameter was 1.9 cm.

The cluster of intense echoes is beginning to bulge eastward at 1351 UTC (near point A in Fig. 8d), but reports of strong wind gusts and hail have ceased. The lack of severe weather reports may be explained by the low population density beneath the convection, but storm surveys also found little evidence of damage.

The echoes reaching from the crest of the LEWP eastward across extreme west Tennessee, point B in Fig. 8d, suggest the downwind (east) extension of convection often found from the northern part of progressive derechos (Johns and Hirt 1987). Smith (1990) associated similar downwind extensions with low-level warm advection, and termed the pattern a "warm advection wing." The inward bulges on the west side of the main echo cluster over east Arkansas (labeled C in Fig. 8d) resemble the weak echo channels (WECs) Przybylinski and DeCaire (1985) identified in bow-echo radar signatures.

Destructive wind gusts (measured at 34 m s^{-1} and estimated up to 45 m s^{-1}) were occurring in the Memphis area at 1450 UTC. The strong winds were near the tight reflectivity gradient at the leading edge of the echoes in Fig. 8e. Only one major WEC remains (A in Fig. 8e); that feature is at the west end of the area where the most destructive wind gusts occurred. The WECs appear to be a result of dry air in a rear-to-front local wind maxima impinging on the back edge of the system (Burgess and Smull 1990). The coincidence of the WEC and subsequent extreme wind gives credence to the theoretical relationship between the phenomena (Przybylinski and DeCaire 1985).

Note the area of lower reflectivity (stippled area) between the strong leading echo and the trailing echoes just west of the WEC in Fig. 8e. The zone of lower reflectivity resembles the "reflectivity trough" described by Testud et al. (1984). Evaporation of precipitation falling from remnants of convective elements may have caused the reflectivity trough (Testud et al. 1984; Smull and Houze 1987) as dry midtropospheric air intruded from the rear of the precipitation complex.

The development of the reflectivity trough may mean dry air is accelerating into the system from its rear, and may indicate the overtaking air can contribute to wind gusts along the leading edge of the squall line (Weisman 1990; Smull and Houze 1987). Numerical simulations using θ_e tracers and Doppler radar observations show a substantial part of the cold outflow from mature systems is derived from a descending rear-to-front flow (Weisman 1990; Johnson et al. 1990; Houze et al. 1989; Burgess et al. 1990; Gao et al. 1989). Bowing along a squall line is where the rear inflow is strongest (Smull and Houze 1987). If it contributes to flow within the cold dome, the rear inflow can be a significant mesoscale feedback (Schmidt et al. 1990). Convergence along the outflow will be strengthened in those circumstances, leading to enhanced convection and faster squall-line propagation.

Figure 8f (1621 UTC) illustrates growth of the trailing reflectivity trough. The stippled area just to the rear of the bow echo in Fig. 8f shows a precipitation-free area. Damaging winds continued to the north and east of the reflectivity trough, and tornadoes occurred near the north end of the bow echo within the following hour. Echoes located south of the rain-free area had nearly identical reflectivity, but produced few damaging wind gusts. WECs continue along the back edge of the bulging squall line at 1621 UTC (A in Fig. 8f).

Figure 8g (1708 UTC) shows a continuation of features described for earlier radar images. The shape of the radar echoes suggests rotation in the weaker reflec-

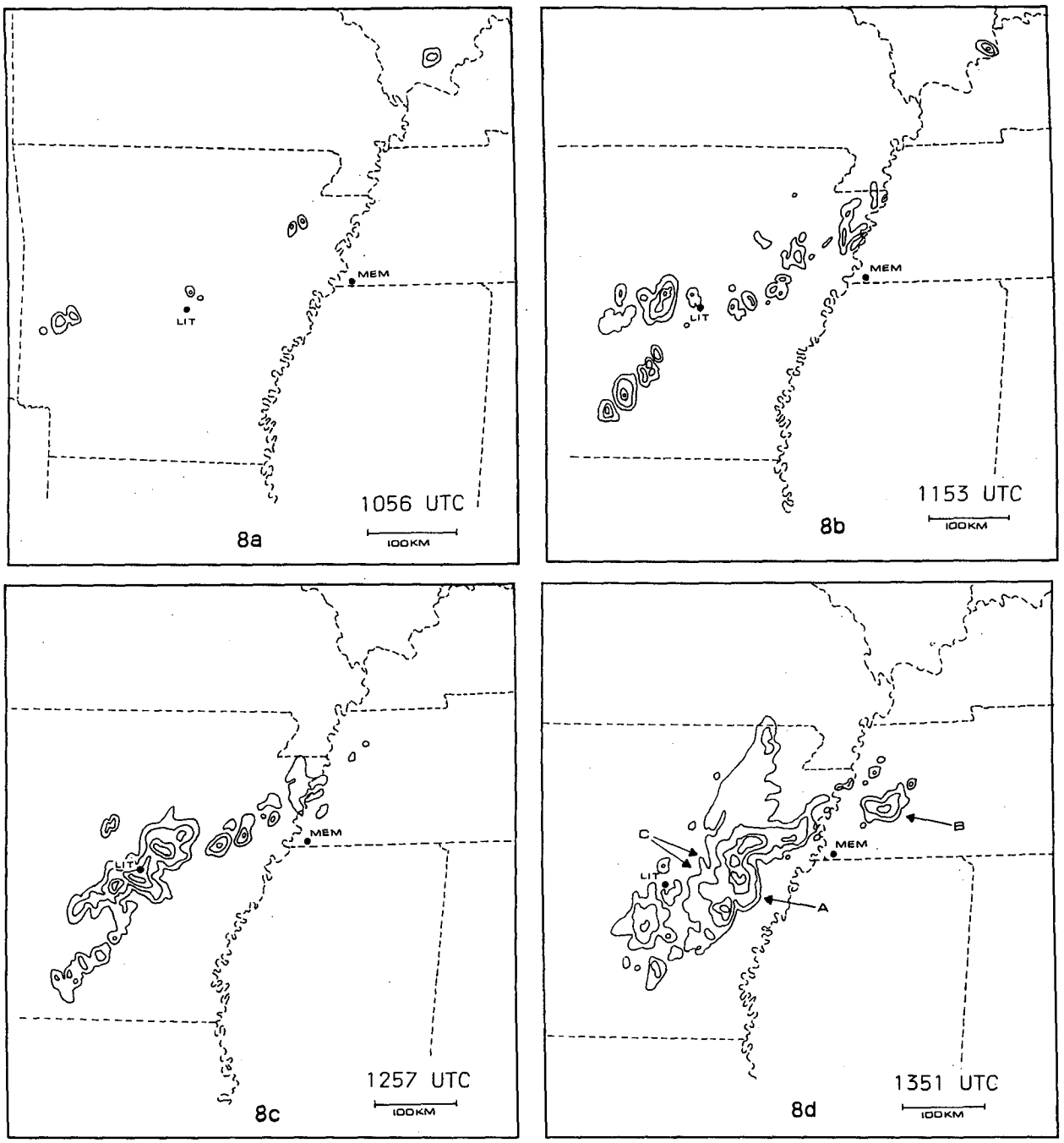

FIG. 8. (a) Radar reflectivity pattern at 1056 UTC 9 April 1991 from the PPI presentation of the Memphis, Tennessee, WSR-74S radar. Contours are NWS VIP levels. Elevation angle 0.5°. Shows isolated convection developing along cold front (see Fig. 3b). (b) Same as (a) except at 1153 UTC. Convection beginning to intensify and move ahead of cold front. (c) Same as (a) except at 1257 UTC. Convection continues to intensify ahead of the cold front. (d) Same as (a) except at 1351 UTC. Eastward bulge at A may indicate echo has started to "bow" outward. (e) Same as (a) except at 1450 UTC. Arrow at A points to major WEC. Damaging winds (measured to 34 m s^{-1}) are occurring at Memphis, Tennessee (MEM), beneath the tight reflectivity gradient just east of the WEC. (f) Composite radar presentation at 1621 UTC, derived from information from the WSR-74S radar at Memphis and the WSR-57 radar at Nashville (BNA). Contours are NWS VIP levels. Arrows at A point to WECs. Stippled area shows a rain-free area immediately to the rear of the bowed-out part of the squall line. (g) Radar reflectivity pattern at 1708 UTC 9 April 1991 from the PPI presentation of the Nashville WSR-57 radar. Contours are NWS VIP levels. Elevation angle 0.5°. Arrow at A points to center of rotation seen in looped radar data. Arrow at B points to major WEC. (h) Same as (g) except at 1735 UTC. Arrow at A points to possible rotation center. (i) Same as (g) except at 1833 UTC. Arrows at A point to some WECs. The stippled area (B–C–D) highlights the rain-free area between the squall line and the trailing precipitation. Arrow at E points to center of possible rotation. (j) Same as (g) except at 1917 UTC.

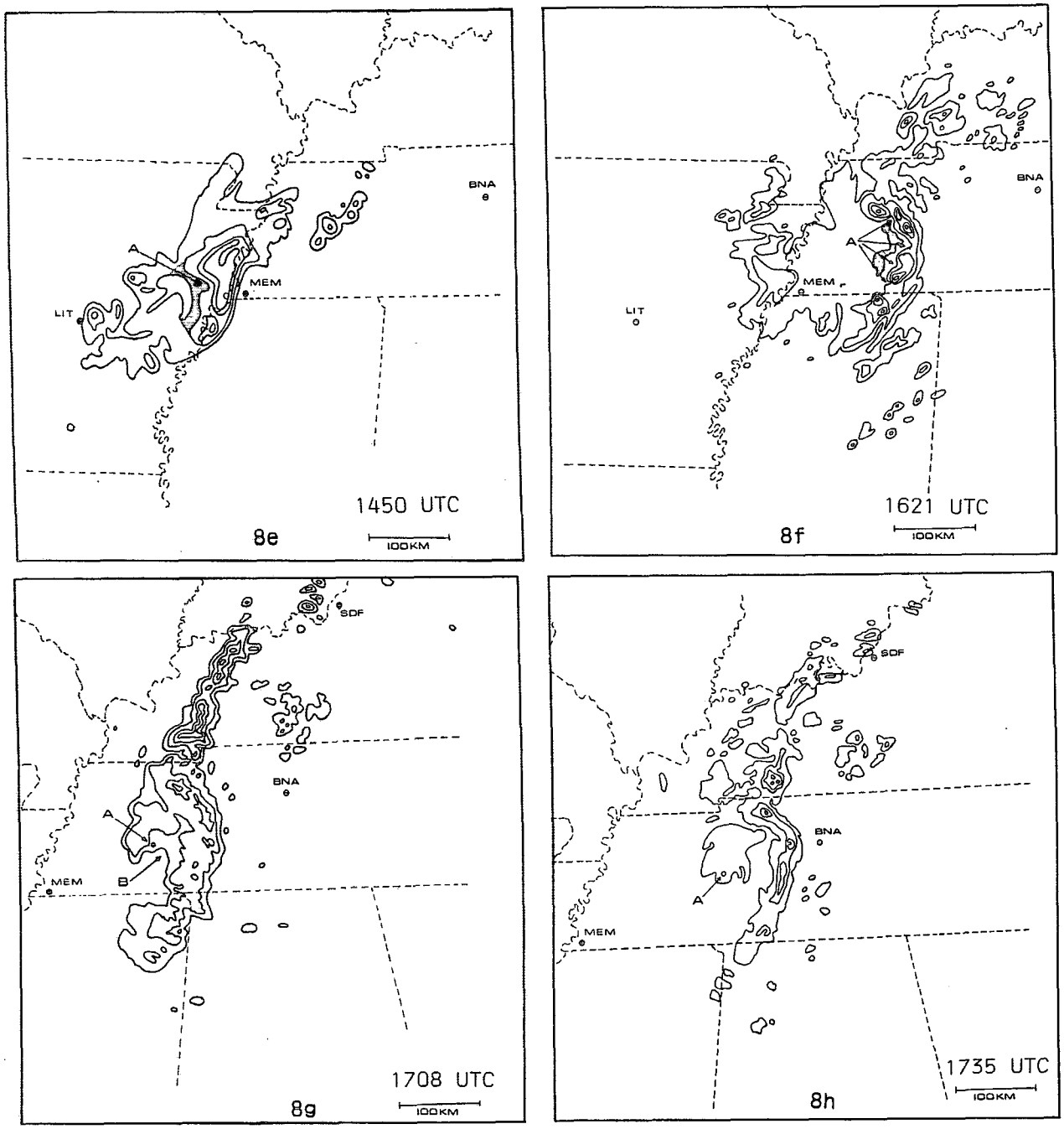

FIG. 8. (*Continued*)

tivities toward the squall line's trailing edge. Indications of rotation are stronger when the archive radar film is viewed sequentially (looped). The apparent rotation center (near point A) is just north and west of the largest weak echo channel (B in Fig. 8g), and suggests a large vortex or mesocyclone in the midlevel precipitation shield trailing the main squall line. Burgess and Smull (1990) reported cyclonic vortices located along the north edge of WECs, while Stirling and Wakimoto (1989) used Doppler radar to confirm rotation implied by conventional radar depiction of similar trailing vortices.

The trailing vortex shape continues in the radar data at 1735 UTC (near point A in Fig. 8h), and the shape of the squall line is characteristic of a mature bow echo. The evolution of the bow echo closely resembles the

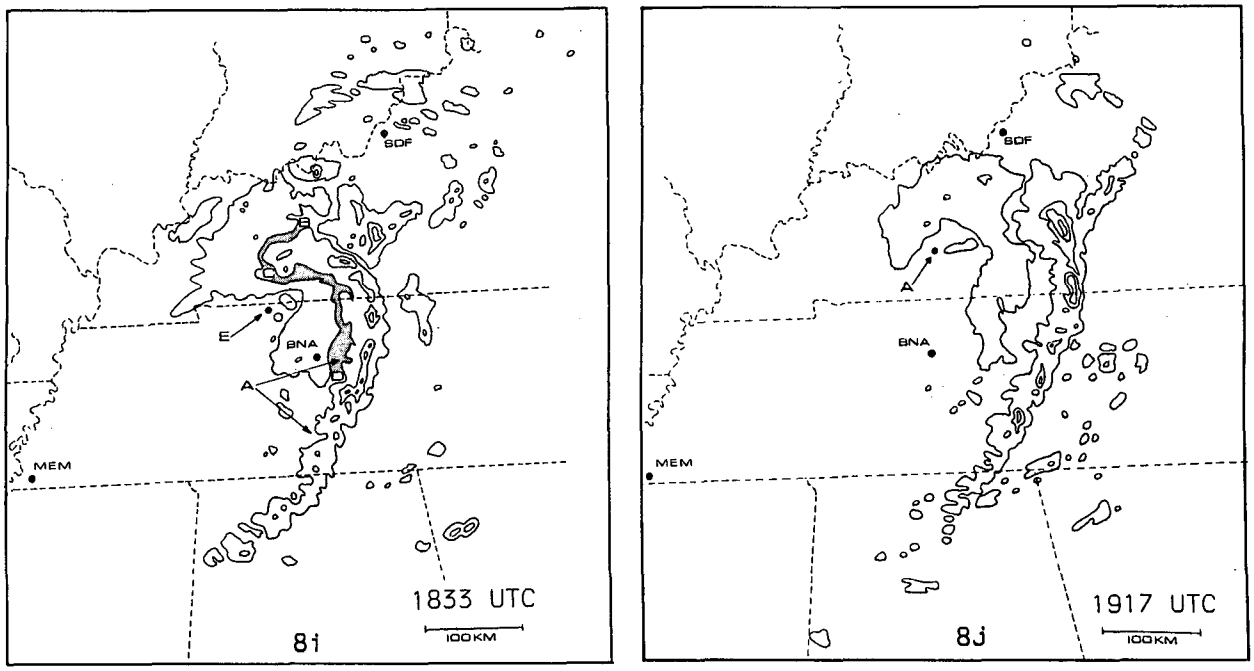

FIG. 8. (*Continued*)

description by Fujita (1978) of the evolution into a comma echo. Destructive winds continue from near the center of the squall line's bulging portion northward, and there were a few tornado reports near the crest of the LEWP.

At 1833 UTC (Fig. 8i), the bow echo is almost completely evolved into a comma echo shape. A suggestion of a trailing circulation (center near point E), WECs (some examples at A in Fig. 8i), and a trough of lower reflectivity (the precipitation-free zone indicated by the stippled area labeled B–C–D in Fig. 8i) are still present. Damaging winds continue during the next hour northward from near the center of the bulging section.

The trailing precipitation area has grown and is quite large in the 1917 UTC radar data (Fig. 8j). Bulging in the squall line has decreased, and the line is straighter. The circulation suggested by the shape of the trailing precipitation echoes appears to have shifted farther north (center near point A in Fig. 8j), relative to the crest of the LEWP. Damaging wind and occasional tornado reports continued to shift toward the north, as well.

5. 9 April 1991 downburst generation mechanisms

As described in section 3, severe thunderstorms first developed in strong moisture convergence ahead of the cold front over central Arkansas about 1100 UTC. Five hours later (1600 UTC), forcing concentrates along the thunderstorm gust front and appears undiminished (Fig. 9). The 1600 UTC surface winds over southwest Tennessee gust from the west at 23 m s^{-1} just west of the gust front, while south winds average 5 m s^{-1} east of the front. The strong convergence produced by this velocity field allows convection to propagate or redevelop along the outflow boundary within the highly unstable air mass.

Not all cases of deep convection cause downbursts and fewer still produce downbursts as strong, widespread, or long-lived as those of 9 April 1991. A sensible question is: What are some of the factors that cause the strong winds associated with this derecho as it de-

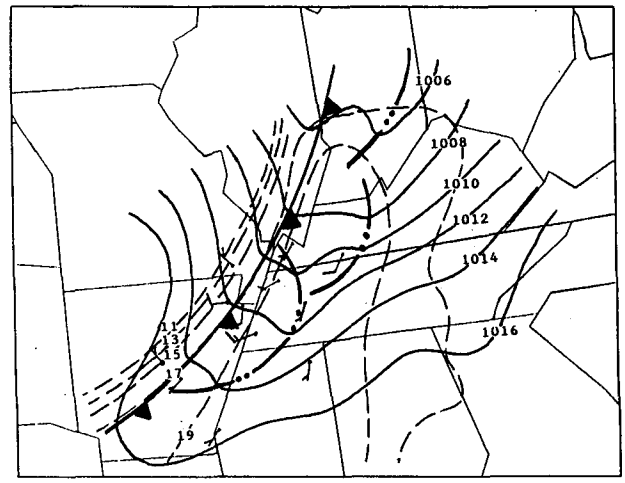

FIG. 9. Same as Fig. 3b except at 1600 UTC. Plotted winds illustrate strong convergence along outflow boundaries. Full wind barbs are 10 m s^{-1}, half-barbs are 5 m s^{-1}.

velops and moves across Arkansas and the west half of Tennessee?

In the case of damaging downdrafts in wet regimes (Atkins and Wakimoto 1991), dry air in the middle troposphere can play a critical role in creating destructive surface winds with convective storms. When strong updrafts penetrate an elevated dry layer, the dry air evaporatively cools as it mixes or entrains with the cloudy updrafts. Equal or greater amounts of cooling will take place where precipitation particles such as rain or hail evaporate as they fall through the dry air. If the temperature cools enough, the chilled air becomes negatively buoyant and accelerates downward. Such downdrafts can be destructive when they strike the earth's surface and spread rapidly in the horizontal.

Downbursts were possible when the 9 April 1991 derecho occurred. High instability characterizes the atmosphere shown in Figs. 6a and 6b. The lower levels are wet and warm; higher levels are cooler and drier. Figure 7 shows surface values of θ_e over the derecho genesis area are at least 20° higher than values 6 km AGL. Atkins and Wakimoto (1991) found similar vertical profiles of θ_e across the southeastern United States on days when damaging surface winds occurred.

Analysis of θ_e also points to a likely elevation source of the downdrafts. Following Knupp and Cotton (1985), we assume the conservative nature of θ_e allows its use as an air parcel tracer. Values of θ_e immediately behind the gust front shown in Fig. 10 range from 320 to 325 K. Comparing these values to Fig. 7 suggests downdrafts sink to the surface from between 3 and 4 km AGL; cooler air with low humidity is found at those altitudes.

Caracena and Maier (1987) provide a way to make a quantitative estimate of how much evaporative cooling contributes to surface wind gusts. That technique was adapted from an approach developed by Foster (1958). Briefly, the methodology is based on the equation of buoyancy-induced vertical motion

$$\frac{dw^2}{dz} = 2\frac{T'_v}{T_v}g, \qquad (1)$$

where w is the vertical velocity, g the acceleration due to gravity, T_v the virtual temperature of the environment, and T'_v the difference between T_v and the virtual temperature of the air parcel undergoing evaporative cooling. It is apparent from Eq. (1) that an air parcel cooler than its surroundings is negatively buoyant and accelerates downward.

Caracena and Maier assume most of a parcel's kinetic energy is conserved. Therefore, when a downburst strikes the ground its maximum horizontal velocity V_m must equal the vertical velocity (w) just prior to impact. From this premise, Eq. (1) can be expanded such that

$$V_m = \left[2\int_0^{\mathrm{LFS}} \left(\frac{T'_v}{T_v}\right) g\,dz\right]^{1/2}, \qquad (2)$$

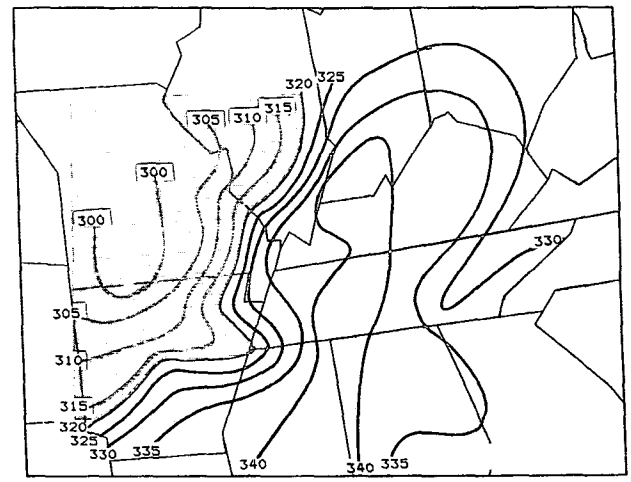

FIG. 10. Same as Fig. 5 except at 1600 UTC. Area with temperatures below 320 K is stippled. Note low θ_e values spreading into southwest Tennessee, immediately behind the outflow boundary shown in Fig. 9. Comparing these values to those in Fig. 7 suggests air in the cold dome had its origin between 3 and 4 km AGL.

where LFS is the level of free sink or source elevation of the downdraft.

Using 1200 UTC rawinsonde information in Eq. (2) with an LFS of 3.5 km AGL (determined from θ_e analysis) yields a V_m of nearly 25 m s^{-1}. Winds were measured at 34 m s^{-1} over southwest Tennessee, and damage estimates suggest velocities up to 45 m s^{-1}. Thus, evaporative cooling can explain most but not all of the surface gust speed.

While evaporative cooling may be considered the greatest factor governing downdraft strength, another possible contributor to the strength of surface outflow can be downward transport of higher momentum possessed by winds in the middle troposphere (Sasaki and Baxter 1988). This downward transfer becomes a factor when parcels in the elevated dry layer conserve their large horizontal speeds as they become negatively buoyant and descend to the surface. Winds in the dry layer (3 to 4 km AGL) over the 9 April 1991 genesis area average 15 to 20 m s^{-1}. That wind velocity can be a source of horizontal momentum when parcels move downward from this elevation.

Wind directions associated with the surface wind gusts suggest a contribution from downward momentum transfer. Without exception, wind velocities during the early evolution of the 9 April 1991 derecho include large westerly components. Gust directions range from 250° to 320°. These directions correspond to winds near the LFS (3.5 km AGL)—260° at 15 to 20 m s^{-1}. In contrast, downbursts that originate where winds aloft are comparatively weak show considerable variability in gust direction. Surface gusts, under those circumstances, radiate from the impact area in a starburst pattern (Wakimoto and Bringi 1988).

Finally, radar reflectivities indicate rainfall rates in

excess of 7.5 cm h^{-1} through a large part of the area experiencing high winds. Precipitation drag or water loading may have therefore been substantial within the thunderstorms and could have played some part in forcing downbursts.

6. Summary and conclusions

Synoptic conditions associated with the 9 April 1991 derecho were, in many respects, unlike those described by studies of warm-season derechos. The absence of an east–west surface boundary, the strength of the approaching midlevel trough, and the absence of low-level moisture pooling were the more obvious differences. Other differences include dryness at 700 mb upstream from the genesis area rather than over and downstream, as is the case for summer derechos; θ_e somewhat lower than warm-season events; and that the 9 April 1991 derecho did not move along the thermal gradient at 700 and 850 mb.

There were similarities to warm-season derechos, however. Similarities include the amount of potential instability over the genesis area and an LFC that sloped downward from the genesis area toward the midpoint of the derecho track. Other similarities are moderately cold air, moderately dry air, and moderately strong winds at midlevels (around 500 mb), and a gradual change from veering wind shear over the genesis area to unidirectional shear eastward along the derecho track.

Similarities between this case and documented warm-season events suggest that some atmospheric conditions associated with summer derechos may be common to derechos in all seasons. Those conditions include abundant moisture at lower levels, a layer of strong (or moderately strong) winds in an elevated dry layer around 500 mb, and a progressively lower level of free convection (LFC) along the track that storms will follow.

Sufficient instability and moisture foster initial thunderstorm development and promote continued convective release. An elevated dry layer provides a source for evaporative cooling and subsequent strong downdrafts (downbursts). Strong winds in the dry layer offer momentum that can be carried to the surface by the downdrafts. The change from veering winds over the genesis area to unidirectional shear over the storm track will promote an evolution from an area of thunderstorms toward a squall-line structure. A gradually lower LFC makes it progressively easy to initiate new convection along the strong surface outflow.

Regardless of the season, forecasters should be alert to the potential for derecho occurrence when those atmospheric conditions are present and thunderstorms are occurring or are possible.

The emergence of new observation tools such as atmospheric wind profilers, automated surface observation platforms, and operational Doppler radars introduce opportunities for large improvement in the detection and forecasting of hazardous phenomena. But potential improvements may be realized only if forecasters have appropriate conceptual models against which to compare the observed information. The warm-season derecho pattern (Johns and Hirt 1987; Johns et al. 1990) offers a useful model on which forecasters may base advisory strategies. Application, however, must involve thoughtful evaluation of differences between existing conditions and those explained by the models.

Even useful models must be modified to fit variations in initial conditions if they are to be applied successfully. Toward that end, we need to continue to note variations between concepts and particular events, and refine our model by explaining variations in physical terms.

Acknowledgments. We offer thanks to Robert Kuessner, Robert Johns, Robert Boyd, and Benny Terry for assistance in data collection, and to Emilio Vigil, Donald Rogers, Richard Coleman, Keith Dodge and especially Robert Johns for helpful comments and criticism of the editorial content.

REFERENCES

Atkins, N. T., and R. M. Wakimoto, 1991: Wet microburst activity over the southeastern U.S.: Implications for forecasting. *Wea. Forecasting,* **6,** 470–472.

Bothwell, P. D., 1985: AFOS Data Analysis Program. NOAA Technical Memorandum. NWS SR-114, Fort Worth, TX, 73 pp.

Burgess, D. W., and B. F. Smull, 1990: Doppler radar observations of a bow echo associated with a long-track severe windstorm. Preprints, *16th Conf. Severe Local Storms,* Kananaskis Park, Alberta, Canada, Amer. Meteor. Soc., 203–208.

Caracena, F., and M. Maier, 1987: Analysis of a microburst in the FACE meteorological mesonetwork in southern Florida. *Mon. Wea. Rev.,* **115,** 969–985.

Foster, B. S., 1958: Thunderstorm gusts compared with computed downdraft speeds. *Mon. Wea. Rev.,* **86,** 91–94.

Fujita, T. T., 1978: Manual of downburst identification for Project NIMROD. SMRP Res. Paper #156, Univ. of Chicago.

Gao, K., and D. Zhang, 1989: The structure and evolution of rear inflow and surface wake lows associated with the 10–11 June 1985 squall line. Preprints, *12th Conf. Weather Analysis and Forecasting,* Monterey, California, Amer. Meteor. Soc., 117–120.

Hart, J. A., and J. Korotky, 1990: The SHARP Workstation v1.50. NOAA, NWS Eastern Region, unpublished report.

Houze, R. A., S. A. Rutledge, M. I. Biggerstaff, and B. F. Smull, 1989: Interpretation of Doppler weather radar displays of midlatitude mesoscale convective systems. *Bull. Amer. Meteor. Soc.,* **70,** 608–619.

Johns, R. H., and W. D. Hirt, 1987: Derechos: widespread convectively induced windstorms. *Wea. Forecasting,* **2,** 32–49.

——, and P. W. Leftwich, Jr., 1988: The severe thunderstorm outbreak of July 28–29 1986 . . . A case exhibiting both isolated supercells and a derecho producing convective system. Preprints, *15th Conf. Severe Local Storms,* Baltimore, Amer. Meteor. Soc., 448–451.

——, K. W. Howard, and R. A. Maddox, 1990: Conditions associated with long-lived derechos—An examination of the large-scale environment. Preprints, *16th Conf. Severe Local Storms,* Kananaskis Park, Alberta, Canada, Amer. Meteor. Soc., 408–412.

Johnson, R. H., W. A. Gallus, and M. D. Vescio, 1990: Near tropopause vertical motions within the trailing stratiform regions of squall lines. Preprints, *16th Conf. Severe Local Storms,* Kananaskis Park, Alberta, Canada, Amer. Meteor. Soc., 669–674.

Klemp, J. B., R. Rotunno, and M. L. Weisman, 1985: Numerical simulations of squall lines in two and three dimensions. Preprints, *14th Conf. Severe Local Storms,* Indianapolis, Indiana, Amer. Meteor. Soc., 179–182.

Knupp, K. R., and W. R. Cotton, 1985: Downdraft initiation within precipitating convective clouds. Preprints, *14th Conf. Severe Local Storms,* Indianapolis, Indiana, Amer. Meteor. Soc., 171–174.

Miller, R. C., 1972: Notes on analyses and severe storm forecasting procedures of the Air Force Global Weather Central. Air Weather Service Tech. Rep. 200 (rev.), Scott AFB IL, 94 pp.

Przybylinski, R. W., and D. M. DeCaire, 1985: Radar signatures associated with the derecho, a type of mesoscale convective system. Preprints, *14th Conf. Severe Local Storms,* Indianapolis, Indiana, Amer. Meteor. Soc., 171–174.

Sasaki, Y. K., and T. L. Baxter, 1986: The gust front. *Thunderstorm Morphology and Dynamics,* University of Oklahoma, 187–196.

Schmidt, J. M., C. J. Tremback, and W. R. Cotton, 1990: Numerical simulations of a derecho event: Synoptic and mesoscale components. Preprints, *16th Conf. Severe Local Storms,* Kananaskis Park, Alberta, Canada, Amer. Meteor. Soc., 422–427.

Shapiro, M. A., 1982: Mesoscale weather systems of the central United States. CIRES/NOAA Tech. Rep., University of Colorado, 78 pp.

Smith, B. E., 1990: Mesoscale structure of a derecho-producing convective system: The southern great plains storms of May 4, 1989. Preprints, *16th Conf. Severe Local Storms,* Kananaskis Park, Alberta, Canada, Amer. Meteor. Soc., 455–460.

Smull, B. A., and R. A. Houze, 1987: Rear inflow in squall lines with trailing stratiform precipitation. *Mon. Wea. Rev.,* **115,** 2869–2889.

Stirling, J., and R. M. Wakimoto, 1989: Mesoscale vortices in the stratiform region of a decaying midlatitude squall line. *Mon. Wea. Rev.,* **117,** 452–458.

Stone, H. M., 1988: Convection parameters and hodograph program—CONVECTA & CONVECTB. NOAA, NWS Eastern Region, unpublished report.

Testud, J., F. Roux, M. Chong, and G. Scialom, 1984: Comparison the dynamical structures of two tropical squall lines observed during "COPT 81" experiment. *22nd Conf. on Radar Meteor.,* Zurich, Switzerland, Amer. Meteor. Soc., 37–42.

Wakimoto, R. M., and V. N. Bringi, 1988: Dual polarization observations of microbursts associated with intense convection: The 20 July storm during the MIST project. *Mon. Wea. Rev.,* **116,** 1521–1539.

Weisman, M. L., 1990: The numerical simulation of bow echoes. Preprints, *16th Conf. Severe Local Storms,* Kananaskis Park, Alberta, Canada, Amer. Meteor. Soc., 428–433.

——, and J. B. Klemp, 1984: The structure and classification of numerically simulated convective storms in a directionally varying wind shear. *Mon. Wea. Rev.,* **112,** 2479–2498.

——, and ——, 1986: Characteristics of isolated convective storms. *Mesoscale Meteorology and Forecasting,* Amer. Meteor. Soc., 331–358.

——, R. Rotunno, and J. B. Klemp, 1990: The role of rear-inflow jets in the production of long-lived meso-convective systems. Preprints, *16th Conf. Severe Local Storms,* Kananaskis Park, Alberta, Canada, Amer. Meteor. Soc., 652–657.

Xue, M., 1990: Toward the environmental conditions for long-lived squall lines: Vorticity versus momentum. Preprints, *16th Conf. Severe Local Storms,* Kananaskis Park, Alberta, Canada, Amer. Meteor. Soc., 146–149.